Applied Surface Science 653 (2024) 159319

Contents lists available at ScienceDirect

Applied Surface Science

journal homepage: www.elsevier.com/locate/apsusc

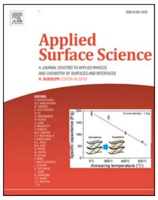

Full Length Article

Defining the nature of adventitious carbon and improving its merit as a charge correction reference for XPS

Lauren H. Grey [a,b], Heng-Yong Nie [a,c,d], Mark C. Biesinger [a,b,d,*]

[a] Surface Science Western, The University of Western Ontario, London N6G 0J3, ON, Canada
[b] Department of Chemistry, The University of Western Ontario, London N6A 5B7, ON, Canada
[c] Department of Physics and Astronomy, The University of Western Ontario, London, N6A 3K7, ON, Canada
[d] Carbon to Metal Coating Institute, Queen's University, Kingston, K7L 3N6, ON, Canada

ARTICLE INFO

Keywords:
X-ray photoelectron spectroscopy
XPS
Adventitious carbon
AdC
Charge reference
Charge correction

ABSTRACT

The chemical nature of adventitious carbon (AdC), a thin layer of carbonaceous material that deposits on the surface of most air-exposed samples and is widely used for charge correction of insulating materials in X-ray photoelectron spectroscopy (XPS), has been investigated by XPS and time-of-flight secondary ion mass spectrometry (ToF-SIMS) on a variety of air-exposed samples from various material classes. The results from this case study show that on average AdC is aliphatic in nature with ~ 25 % of carbon species having bonds to oxygen. D-parameter and ToF-SIMS results show that AdC is not graphitic in nature, as had been suggested in earlier studies. Using assumptions about volatile organic compounds (VOC) in air that contribute to AdC accumulation, a peak-fitting model for the C 1 s XPS spectrum of AdC including beta shifted carbon peaks was developed. This model is shown to increase accuracy of the positioning of the aliphatic peak. Using this model and data from 117 samples an AdC C 1 s aliphatic peak binding energy of 284.81 eV (+/-0.25 eV) was found. Average XPS and ToF-SIMS AdC spectra are presented. The average AdC XPS spectrum has been utilized to model the C 1 s spectrum of complex organic compounds with AdC present.

1. Introduction

Analysis of insulating materials by X-ray photoelectron spectroscopy (XPS) is complicated by the need to use a charge correction method to compensate for the action of the electron flood gun or other charge neutralization systems. Sample charging effects and the use of charge neutralization in XPS has been discussed at lengths elsewhere. [1,2,3,4,5,6,7,8].

A number of charge correction procedures are available; however, the use of adventitious carbon (AdC) is one of the most common and, in many cases, the only option available. This is done by fitting the carbon 1 s (C 1 s) spectrum of adventitious carbon with synthetic components and then adjusting the binding energy (B.E.) scale of all spectra so the lowest energy component of the C 1 s spectrum (attributed to aliphatic carbon) is set to a standardized value. This value has had a significant range in the literature[9], and a consensus on its position from the XPS community is needed to make this a better charge correction procedure. ASTM E1523-15[10] notes a range of 284.6 eV to 285.2 eV from reported literature sources (section 7.3.1.2) but suggests 284.8 eV as a common reference value (section 7.3.1.1). Databases such as that from NIST[11] also use 284.8 eV as the accepted standard. This charge correction method is convenient and easy to implement as adventitious carbon is found on the surface of most air-exposed samples.

Although the use of adventitious carbon is one of the most popular methods for charge correction in XPS, there has been some controversy regarding its use. Greczynski and Hultman have written multiple papers that outline their apprehensions surrounding the use of adventitious carbon as a charge reference. The reader is directed to their work[9] which gives account of AdC usage concerns dating back to the 1970s. Specifically, they and others cite concerns about the unknown chemical composition of the AdC layer, the position of the aliphatic component of the AdC spectrum, and AdC's origin or source.[12].

There has only been one major paper published almost 30 years ago on the chemistry of AdC. In their paper, Barr and Seal used XPS to examine the C 1 s spectra of graphite and hydrocarbon polymers in an attempt to provide a chemical description of AdC.[13] They concluded that adventitious carbon predominately consists of hydrocarbon polymers that contained approximately 10–30 % oxygen-functionalized

---

[*] Corresponding author at: Surface Science Western, The University of Western Ontario, 999 Collip Circle, Suite LL31, London N6G 0J3, Ontario, Canada.
E-mail address: biesingr@uwo.ca (M.C. Biesinger).

https://doi.org/10.1016/j.apsusc.2024.159319
Received 17 August 2023; Received in revised form 7 December 2023; Accepted 4 January 2024
Available online 17 January 2024

Table 1
Average D-parameter values of standard samples and adventitious carbon samples on a variety of surfaces (error: ±0.7 eV).

Sample	D-parameter
Polyethylene (cleaned)	13
Graphite (cleaned)	22.5
AdC on tin	14.5
AdC on titanium	13
AdC on aluminum foil	14.5
AdC on aluminum oxide powder	14.5
AdC on boron powder	13.5
AdC on iron powder	12.5
AdC on silicon wafer	13.5

Table 2
D-parameters of as received and gas cluster ion source sputter cleaned samples of graphite and polyethylene terephthalate (PET) (error: ±0.7 eV).

Sample	Condition	D-parameter
Graphite	As received	21
Graphite	Sputtered	22.5
PET	As received	14
PET	Sputtered	15

Table 3
Vapour pressure at 25 °C for various four and five carbon molecules from reference 26.

Name	# of Carbons	Type	P_v (kPa)
Butane	4	Hydrocarbon	242
Diethyl ether	4	Ether	71.7
Pentane	5	Hydrocarbon	68.3
Ethyl propyl ether	5	Ether	24.2
Butanal	4	Aldehyde	15.7
2-Butanone	4	Ketone	12.6
Ethyl acetate	4	Ester	12.6
Ethyl propanoate	5	Ester	4.97
2-Pentanone	5	Ketone	4.97
3-Pentanone	5	Ketone	4.72
Pentanal	5	Aldehyde	4.58
Methyl butanoate	5	Ester	4.3
2-Butanol	4	Secondary alcohol	2.32
3-Pentanol	5	Secondary alcohol	1.1
1-Butanol	4	Primary alcohol	0.86
2-Pentanol	5	Secondary alcohol	0.804
1-Pentanol	5	Primary alcohol	0.259
Butanoic acid	4	Carboxylic acid	0.221
Pentanoic acid	5	Carboxylic acid	0.024

carbons. While this is a start, it does not answer many questions that arise about adventitious carbon. This paper aims to present more data on the chemical nature of AdC.

In addition to the AdC aliphatic component position issues (standardized B.E. value) discussed above, another long-claimed characteristic of adventitious carbon is that it is graphitic in nature. Barr and Seal's paper attempted to disprove this in a qualitative fashion (i.e. through analysis of spectral shape),[13] but this technique is more intuition-based, which is not sufficient when it concerns the validity of methodology. This study, instead, will use the more quantitative D-parameter method to determine the hybridization of the carbon. The D-parameter, first reported by Lascovich and colleagues,[14] describes the difference between the minimum and the maximum of the first derivative of the carbon Auger spectrum. This value has been shown to be linearly correlated to the percentage of sp^2 versus sp^3 hybridized carbon.[15] D-parameter data will prove that AdC is not graphitic in nature and demonstrate that 284.5 eV (the B.E. of graphitic carbon) is not an appropriate value for charge referencing value for AdC.

The most likely origin/source of most adventitious carbon is from the atmosphere (although Greczynski and Hultman have shown that organic molecules volatilizing from sample containers can also influence AdC composition[16]). Various studies in the field of environmental chemistry have looked into volatile organic compounds (VOCs) present in the atmosphere at various locales.[17,18,19,20,21,22,23,24] The European Union defines VOCs as "any organic compound having, at 293.15 K, a vapour pressure of 0.01 kPa or more".[25] While most published papers look into compounds such as benzene, chloroform, styrene, formaldehyde, Freon, and short-chain hydrocarbons, which can affect air quality and human health, there are many other examples of organic compounds that are VOCs. While some organic compounds are more volatile than others, many four, five, and six carbon organic compounds have a vapour pressure larger than 0.01 kPa at 20 °C,[26] making them more likely to be present than higher carbon number containing compounds. Vapour pressure data shows that, generally, the volatility of organic compounds is as follows: hydrocarbons > ethers > aldehydes, ketones, esters > alcohols > carboxylic acids. Volatility also decreases as overall molecule size increases. With the exception of pure hydrocarbons, few compounds with 10 or more carbons are volatile at standard atmospheric temperature and pressure. This basic knowledge informs our conclusions about adventitious carbon and assists with assumptions to help build more accurate peak-fitting models for AdC.

It should be noted that, depending on their origin, the samples showing AdC in this study have been exposed to a mix of atmospheres including: 1) our specific XPS or ToF-SIMS instrument vacuum systems, 2) our facility 3) other Western University laboratories and offices, 4) and supplier warehouses, manufacturing sites, and research institutions from Canada and USA. AdC accumulation in different parts of the world may have differing chemistries, particularly if local conditions include high concentrations of specific VOCs.

This work cross-references XPS findings with time-of-flight secondary ion mass spectrometry (ToF-SIMS) data. ToF-SIMS uses a focused ion beam to ionize and fragment the molecules on a sample surface. These secondary ions are accelerated by an electric field towards a detector that measures their velocity, from which we can determine the mass and identity of the ion fragments. The surface sensitivity of this technique (outermost 1–3 nm) makes it an excellent complement to XPS and very well suited to the study of adventitious carbon. ToF-SIMS users routinely utilize mass fragments (e.g. CH_3^+, CH^-, C_4H^-, and $C_3H_5^+$) from AdC on sample surfaces for mass calibration purposes.

These techniques have allowed for a determination of the hybridization of AdC via the D-parameter and ToF-SIMS spectral comparison. We also present a novel fitting model for adventitious carbon and evidence that this model increases the accuracy of charge referencing with AdC by fine-tuning the position of the aliphatic peak. This analysis, building on previous work,[27] also adds further justification for the positioning of the hydrocarbon component of AdC at 284.8 eV in the C 1 s spectrum. Finally, this work compares the chemical composition of adventitious carbon on different types of materials and presents an average adventitious carbon spectrum for analysis of complex organic materials. These pieces of evidence combined should lend more merit to the adventitious carbon charge referencing technique and address concerns about the suggested unknown nature of AdC.

2. Materials and methods

2.1. Sample Selection, Handling, Preparation, and mounting

It was important to select a variety of types of substrates for this study because one significant concern surrounding adventitious carbon is that its composition may vary on different substrates, leading to less accurate charge referencing. Most previous studies have been carried out on only conductive metallic based surfaces (sputter cleaned or air-oxidized surfaces).[28,29,30] We prioritized looking at substrates of various material classes, such as metals, glass, ceramics, metal and non-metal powders, and semiconductors. We were also careful to choose samples that did not contain intrinsic carbon, as this would affect our

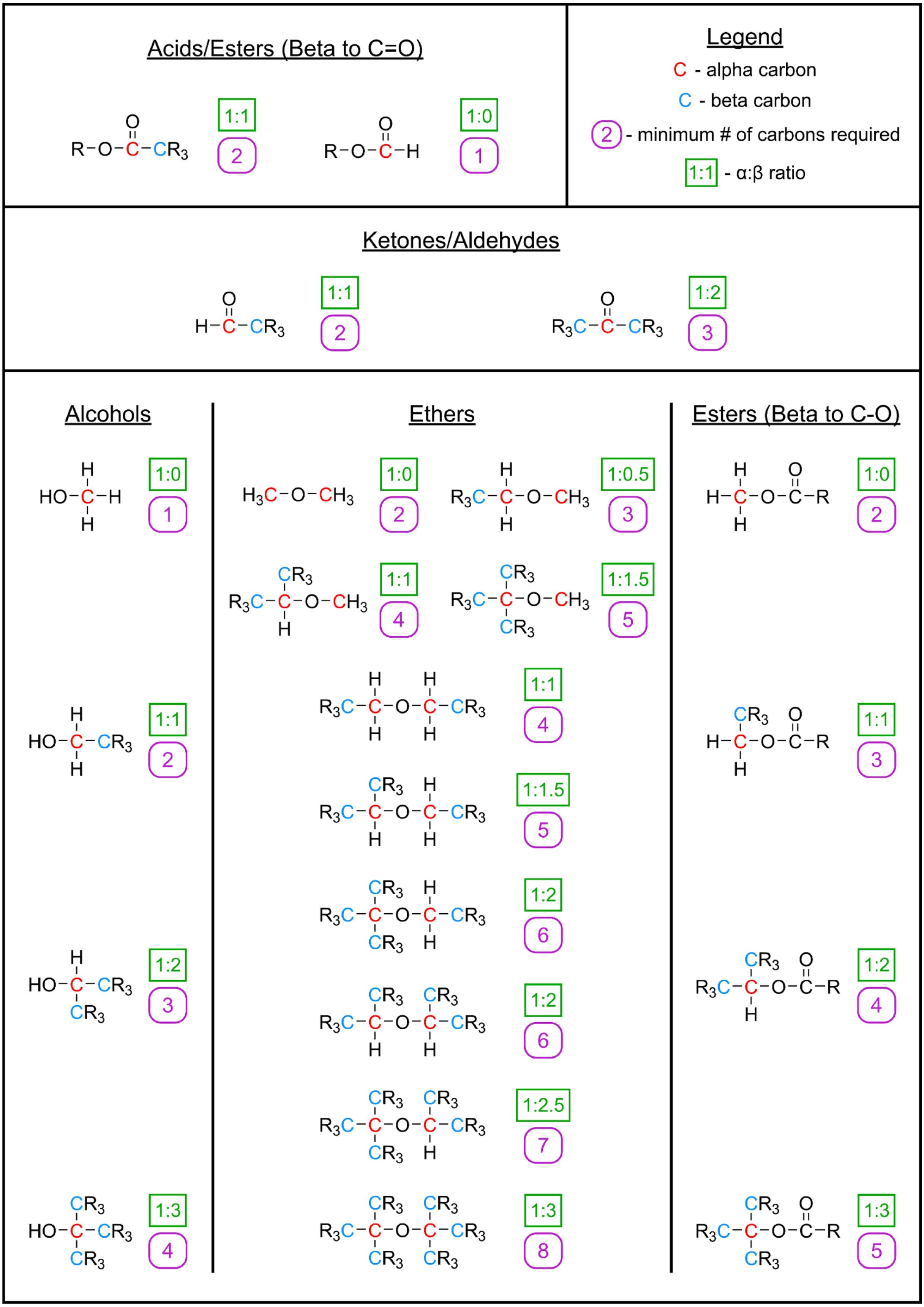

Fig. 1. All functional group possibilities considered when creating the beta peak adventitious carbon fitting model, including alpha to beta peak area ratios and minimum number of carbons required (in the molecule) for each combination.

Table 4
Curve-fitting parameters for adventitious carbon (C 1 s) including shifted beta peaks (*). Lineshape for all peaks is 30 % Lorentzian, 70 % Gaussian (GL(30) in CasaXPS). Note that the areas for peaks A, B, C, and D should be left unconstrained.

Species	Peak Identifier	Starting Position (eV)	Common Range (eV)	FWHM (eV)	Area (CPS*eV)
C–C, C–H	A	284.8		0.7–1.5	A
C-O	B	A + 1.5	A + 1.3 to A + 1.7	A*1	B
C = O	C	A + 3	A + 2.8 to A + 3.0	A*1	C
O-C = O	D	A + 4	A + 3.8 to A + 4.3	A*1[#]	D
C*-C-O	E	A + 0.2		A*1	B*1.25
C*-C = O	F	A + 0.4		A*1	C*1.5
C*-(C = O)-O	G	A + 0.4		A*1	D*1

[#] Note if this peak-shape is well defined the FWHM constraint can be removed.

ability to interpret the AdC C 1 s spectrum.

Great care was taken to avoid surface contamination of samples, especially since we were interested in looking at adventitious carbon. We chose samples that were stored using the cleanest methods possible (for example, stored in a PET case rather than an open paper package, in glass vials, loosely wrapped in aluminum foil. etc.). When possible, a surface was chosen that was inaccessible to contamination from handling prior to analysis (for example, within a roll of PET or BOPP films inaccessible to fingerprints, inner surface of a glass tube, etc.). Best practices for sample handling and preparation (as described by Stevie et. al[31]) were followed wherever possible. Where breaking of the sample was required, the surface was wrapped loosely in aluminum foil to prevent contamination.

For XPS, graphite was mounted to the sample holder using a carbon adhesive disk and copper tape. All other metallic and non-metal samples and powders were mounted on a glass slide or with non-conductive double-sided tape ("floated") to electrically isolate the sample from the ground and mitigate differential charging.

For ToF-SIMS, solid samples were mounted using copper tape, with care taken to ensure each surface was as flat as possible. Powders were pressed between two pieces of aluminum foil to deposit a thin layer of sample onto the foil. The foil was then mounted on the sample holder using copper tape.

2.2. XPS measurements

The XPS analyses were carried out with a Kratos Axis Supra spectrometer using a monochromatic Al Kα source (15 mA, 15 kV). The instrument work function was calibrated to give a binding energy (B.E.) of 83.96 eV for the Au $4f_{7/2}$ line for metallic gold and the spectrometer dispersion was adjusted to give a B.E. of 932.62 eV for the Cu $2p_{3/2}$ line of metallic copper. The instrument base pressure was 1 × 10^{-9} Torr or better. The Kratos charge neutralizer system was used for analyses as needed (insulating, mixed conducting/insulating, and electrically isolated samples). The Kratos charge neutralization system uses a coaxial low energy electron source within the field of the magnetic lens. The effectiveness of the charge neutralizer was gauged by monitoring the C 1 s spectrum. A sharp main peak with no lower binding energy structure is generally expected.

Survey spectra were recorded using a pass energy of 160 eV and a step size of 1 eV. For C 1 s high-resolution spectra, a 20 eV pass energy and a 0.1 eV step size were used. For C KVV high-resolution spectra, an 80 eV pass energy and a 1 eV step size were used. All spectra were taken using an analysis area of ≈ 300 µm × 700 µm and a 90° electron take-off angle.

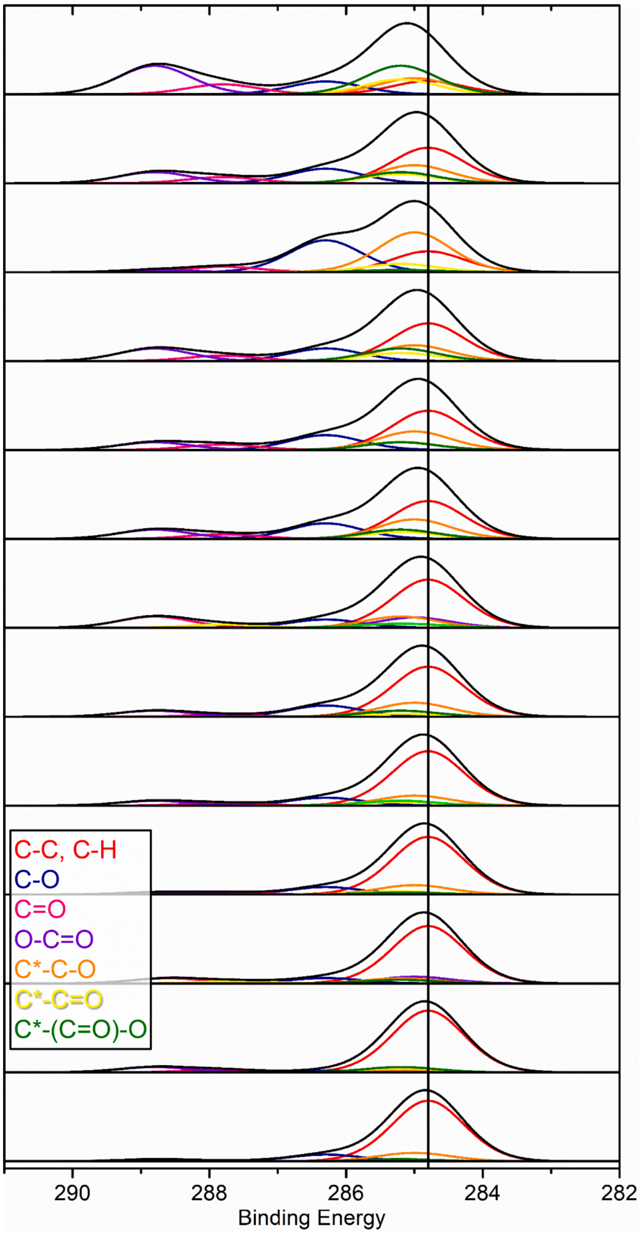

Fig. 2. Simulated adventitious carbon spectra from a variety of surfaces fit using the beta peak model. The vertical black line shows 284.8 eV. Note that as more oxygen functionality is present the peak maximum of the spectrum shifts to higher binding energy as compared to the position of the aliphatic peak at 284.8 eV. Spectra are ordered with most oxygen functionality at the top to least at the bottom.

Ion sputtering of graphite and polymer samples was carried out using a 5 keV Ar^{+}_{3000} gas cluster ion source (GCIS) (3.0 mm × 3.0 mm) for a 30 s interval.

Spectra taken for D-parameter analyses, the complex organic sample C 1 s spectrum (Fig. 4), and the AdC C 1 s spectrum on titanium (Fig. 7) were analyzed using CasaXPS software (version 2.3.26).[32] Spectra were charge corrected so as to have the aliphatic peak (C–C) of adventitious carbon aligned at 284.8 eV. Adventitious carbon was generally fit according to the parameters described by Biesinger,[27] except in cases where beta carbons were accounted for, for which beta shift procedures derived from Beamson and Briggs' polymeric reference data were used.[33] A Shirley background was employed for C 1 s peak-fitting and a 70 % Gaussian / 30 % Lorentzian product formula was used for individual

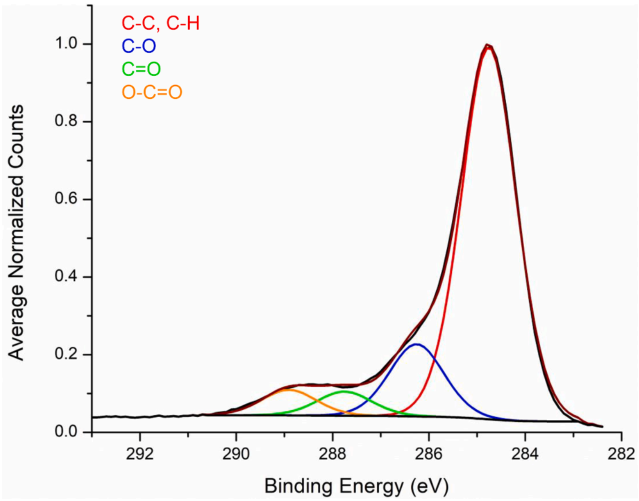

Fig. 3. Average of 80 adventitious carbon C 1 s XPS spectra.

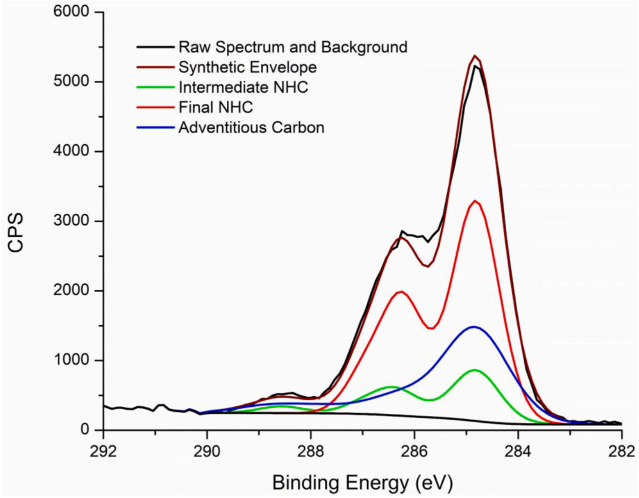

Fig. 4. The C 1 s spectrum of a complex organic sample [36] fit using the average adventitious carbon spectrum.

Table 5
Average adventitious carbon (C 1 s) fitting parameters from an average of 80 AdC spectra.

Component	C–C, C–H	C-O	C = O	O-C = O
Position	A	A + 1.5	A + 3	A + 4.15
% Area	74.8	14.7	5.1	5.5
FWHM	1.33	1.33	1.33	1.33

Table 6
Atomic percent of carbon associated with adventitious carbon for a mixed complex organic sample, calculated using various methods.

Description	Atomic % of carbon from AdC
Calculated according to the known ratio of C:O in sample and survey spectrum	28
Calculated according to the known ratio of C:N in sample and survey spectrum	23
Amount according to C 1 s spectrum fit with average AdC spectrum	28

peaks (defined as GL(30) in CasaXPS).

For the D-parameter calculation, the C KVV spectrum was smoothed, then differentiated. The D-parameter is calculated as the kinetic energy difference between the spectral minimum and maximum of the first derivative of the carbon Auger peak. For more information on D-parameter calculations, see Morgan.[15].

2.3. Five-Year Multi-User facility C 1 s spectral Dataset[27]

The present study makes use the dataset from reference [27]. This dataset was from 1237 samples submitted to a multi-user facility over a five-year period and was used to explore various types of charge correction strategies and their effectiveness. Samples are from a broad range of classes and origins, and a full accounting and description of the dataset is available in the original publication and its associated supplementary data section. 522 of the samples surveyed used AdC for charge-referencing purposes. 80 of these samples are used in the calculation of the average AdC spectrum (Section 3.3). In 117 of these 522 samples where AdC was used for charge referencing, a possible secondary internal charge reference was also available. These secondary references were used to assess the deviation of the aliphatic C 1 s signal from the 284.8 eV standard value used (Section 3.2).

2.4. ToF-SIMS measurements

The samples were examined using an IONTOF (GmbH) TOF-SIMS IV equipped with a Bi cluster liquid metal ion source using a BiMn emitter. The base pressure of the analytical chamber was ~ 1 × 10^{-7} mbar. A pulsed 25 keV Bi_3^+ cluster primary ion beam was used to bombard the sample surface to generate secondary ions. The secondary ions were extracted from the sample surface, mass separated and detected via a reflectron-type time-of-flight analyser, allowing parallel detection of ions having a mass/charge ratio (*m/z*) up to ~ 900 within each cycle (100 μs). A pulsed, low energy electron flood was used to neutralise sample charging. Negative and positive secondary ion mass spectra were collected at 128 × 128 pixels over an area of at least 130 μm × 130 μm. The mass resolutions of $C_2H_5^+$, $C_4H_7^+$, C_2H^- and C_4H^- were 5491, 6470, 4375, and 5245, respectively.

Spectra were analyzed using the SurfaceLab 7 software (IONTOF GmbH, Münster, Germany). The positive ion mass spectra were initially calibrated using H^+, CH_3^+ and $C_3H_5^+$, while negative mass spectra used H^-, CH^- and C_4H^-. More peaks were added to the calibration as needed to achieve more accurate calibration.

Each spectral area was divided into four regions of interest (ROI) to increase the number of duplications and mitigate geometry effects. Where geometry was a concern, each ROI was calibrated and processed separately. Positive ions of interest included $C_xH_y^+$ ions and $C_xH_yO^+$ ions. Negative ions of interest included C_x^-, C_xH^-, and $C_xH_yO_z^-$ ions. Only fragments up to seven carbons were considered, as larger fragments had very little signal.

Principal component analysis (PCA) was performed using NB toolbox (v. 2.9)[34] run in MatLab version R2019b (The MathWorks Inc., Natick, Massachusetts). PCA of positive and negative ions were performed separately. All spectra were normalized to total selected ion intensity and mean-centered prior to analysis. This means that each ion intensity was divided by the sum of the total selected ion intensities, then the column mean was subtracted from each column (forming a matrix where each column has a mean of zero).[35].

3. Results and discussion

3.1. The D-parameter

The D-parameters of all non-potassium containing samples were calculated, as the K LMM Auger peak overlaps with the C KVV peak and interferes with the calculation. An average of two values are reported for

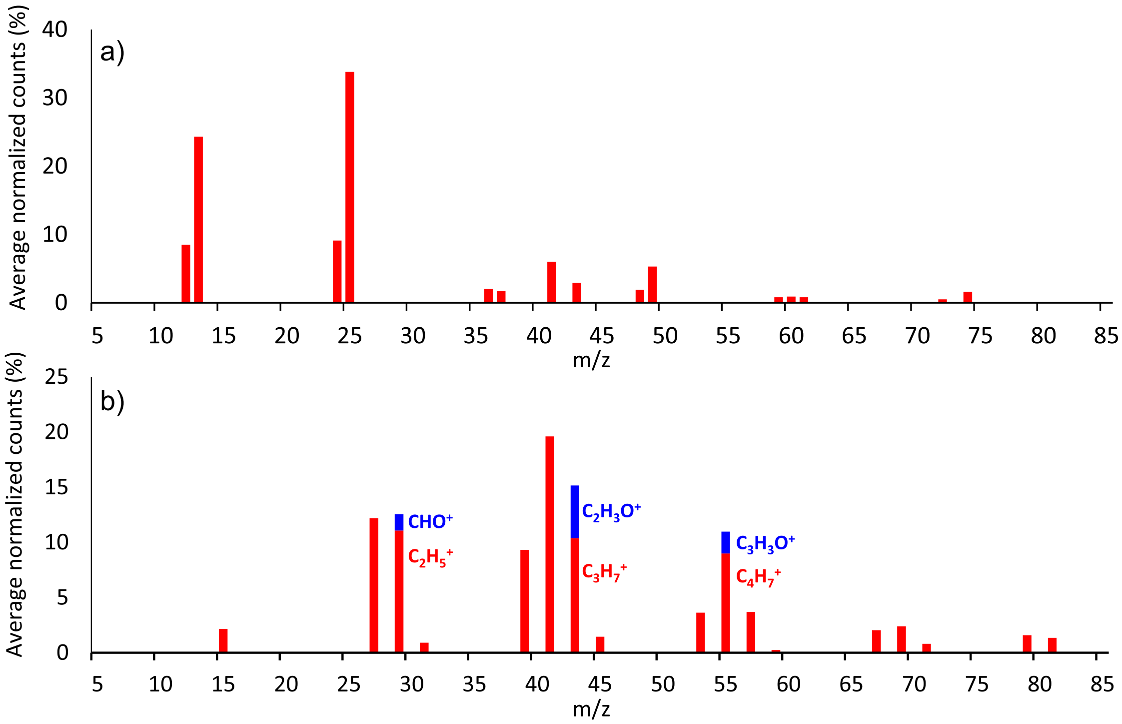

Fig. 5. Average ToF-SIMS adventitious carbon spectra, displayed as line spectra for clarity purposes, for a) negative and b) positive secondary ions.

each sample. The results of the standards (sputtered graphite and polyethylene) compared to the adventitious carbon samples are shown in Table 1.

All adventitious carbon samples had D-parameter values that indicated mostly saturated carbon chains. This is as expected, as adventitious carbon has generally been considered to be composed of mostly aliphatic hydrocarbons. These results provide concrete evidence of the alkane-like nature of AdC and disputes past claims of a graphitic character. Most of the adventitious carbon samples had a slightly higher D-parameter value than polyethylene, which may be due to the sp^2 nature of carbonyl-associated carbons.

In subsequent experiments, sp^2-carbon containing substrates were analyzed before and after ion sputter cleaning via GCIS. As seen in Table 2, the samples with adventitious carbon on the surface had a lower D-parameter than cleaned samples. This indicates that adventitious carbon is decreasing the D-parameter due to its sp^3-hybridized nature. These findings again disprove earlier hypotheses that suggested that AdC may be comprised of graphitic carbon.[4,28] Figures showing selected C KVV spectra and C KVV (first derivative) spectra from samples in Tables 1 and 2 are presented in the supplementary data section (S1 and S2).

3.2. Beta carbon shifts

The traditional adventitious carbon peak fitting model contains four peaks: aliphatic carbons (C–C, C–H), singly-bonded oxygen functionalities (C-O), carbonyl groups (C = O), and carboxyl groups (O-C = O). Each of the carbons associated with these oxygen functionalities may have one or more beta carbons, which will also have a slight chemical shift, according to Beamson and Briggs.[33] Note that, in this context, the alpha carbon is the carbon directly attached to the oxygen, and the beta carbon is attached to the alpha carbon. For simplicity, these shifted beta atom peaks are generally not included in AdC XPS fitting. We present here a new procedure for fitting adventitious carbon that accounts for both alpha and beta shifted carbon atoms.

The model was partially based upon various assumptions about organic compounds in air that could contribute to the formation of AdC. Table 3 shows vapour pressure data for various four and five carbon species. This data, as well as data for six and seven carbon species, demonstrate two important points: (1) ketones and aldehydes are approximately equally as volatile, and (2) as molecule size increases, volatility decreases. Studies on VOCs support the second conclusion, as they report that concentrations of hydrocarbons in the air generally decrease as the molecules get larger.[18,19] In general, this limits the possible amount of beta carbons in volatile organic compounds.

Carboxyl functional groups (organic acids and esters) generally only have one beta carbon per alpha carbon, so setting the beta peak area equal to the alpha peak area is appropriate. Formate esters are one exception to this rule, as they have no beta carbons, but we consider their contribution as VOCs to be small and neglect their contribution for simplicity.

Since ketones and aldehydes are approximately equally as likely to be present in the atmosphere, we took an average of the alpha to beta carbon ratios as their beta peak area. Ketones have a 1:2 alpha to beta carbon ratio and aldehydes have a 1:1 ratio, so we determined that 1.5 times the C = O peak area would be suitable.

C-O functionalities have many more possible configurations than the previous two functional groups. A C-O functionality could have an alpha to beta carbon ratio of 1:0.5, 1:1, 1:1.5, 1:2, 1:2.5, or 1:3. The exact types of functionalities that are present will likely depend on the location and climate of storage,[18] the type of storage container,[16] and other factors that are highly variable. For the sake of convenience and usability, we decided to use various observations and assumptions about VOCs and C-O functionalities to choose one factor for the C-O beta peak area. It is important to note that it is much less important for this peak area to be exact, as it has a much smaller chemical shift than C*-C = O and C*-(C = O)-O and, therefore, it has less of an impact on the shift of the C–C/C–H peak position (note C* is the beta C).

Fig. 1 illustrates all of the possible functional group combinations that we considered when creating this model. The most prominent observation is that compounds with more beta carbons per alpha carbon must contain more carbon atoms. For example, a 1:3 ratio of alpha to beta carbons contains, at a minimum, four carbon atoms. As stated earlier, the likelihood of these compounds being present in air decreases

Table 7
Ion fragments (nominal mass and percent of total selected ions) for the average (140 spectra from 13 samples) ToF-SIMS adventitious carbon spectra for a) negative ions and b) positive ions.

a)		
Negative Ion	Nominal Mass (u)	% Total Selected Ion
C^-	12	8.5
CH^-	13	24.3
C_2^-	24	9.1
C_2H^-	25	33.8
CHO^-	29	0.1
CH_3O^-	31	0.1
C_3^-	36	2.0
C_3H^-	37	1.7
C_2HO^-	41	6.0
$C_2H_3O^-$	43	2.9
C_4^-	48	1.9
C_4H^-	49	5.3
$C_2H_3O_2^-$	59	0.8
C_5^-	60	0.9
C_5H^-	61	0.8
C_6^-	72	0.5
C_6H^-	73	1.6
All above ions	–	100
b)		
Positive Ion	Nominal Mass (u)	% Total Selected Ion
CH_3^+	15	2.2
$C_2H_3^+$	27	12.2
CHO^+	29	1.5
$C_2H_5^+$	29	11.1
CH_3O^+	31	0.9
$C_3H_3^+$	39	9.3
$C_3H_5^+$	41	19.6
$C_2H_3O^+$	43	4.8
$C_3H_7^+$	43	10.4
$C_2H_5O^+$	45	1.4
$C_4H_5^+$	53	3.6
$C_3H_3O^+$	55	2.0
$C_4H_7^+$	55	9.0
$C_4H_9^+$	57	3.7
$C_3H_7O^+$	59	0.2
$C_5H_7^+$	67	2.0
$C_5H_9^+$	69	2.4
$C_5H_{11}^+$	71	0.8
$C_6H_7^+$	79	1.6
$C_6H_9^+$	81	1.3
All above ions	–	100

significantly as molecule size increases. Groups with two or three beta carbons per alpha carbon are, therefore, less available to deposit on the surface. Given this information, it is likely that an area constraint of less then two beta carbons to one alpha (C-O) carbon is applicable.

Testing was carried out with 1:1, 1:1.25, and 1:1.5 ratios using test data from reference 27. Adventitious carbon spectra were fit with each set of fitting parameters and secondary checks were performed. All C–C/C–H peaks had very similar shifts from 284.8 eV as a standard aliphatic peak position (on average 0.02, 0.01, and 0.00 eV respectively). Further results from this process will be discussed later in this section. During this experiment, a factor of 1.5 would, in rare cases where the amount of C-O functionality was large, cause the C–C peak to disappear entirely. While this could be possible in some cases, this is likely not an accurate depiction of most adventitious carbon samples, as one would expect at least some number of hydrocarbons on the surface due to their relative abundance in the atmosphere. Also, given the number of examples in Fig. 1 that have a larger number of beta carbons per alpha carbon, it is unlikely that 1:1 would be the most accurate ratio. Therefore, a factor of 1.25 times the C-O peak area was chosen.

Table 4 describes the procedure used to fit adventitious carbon with both alpha and beta carbons. While using this procedure is not absolutely necessary, one may desire to use it if they are trying to remove as much error as possible in the position of the aliphatic peak.

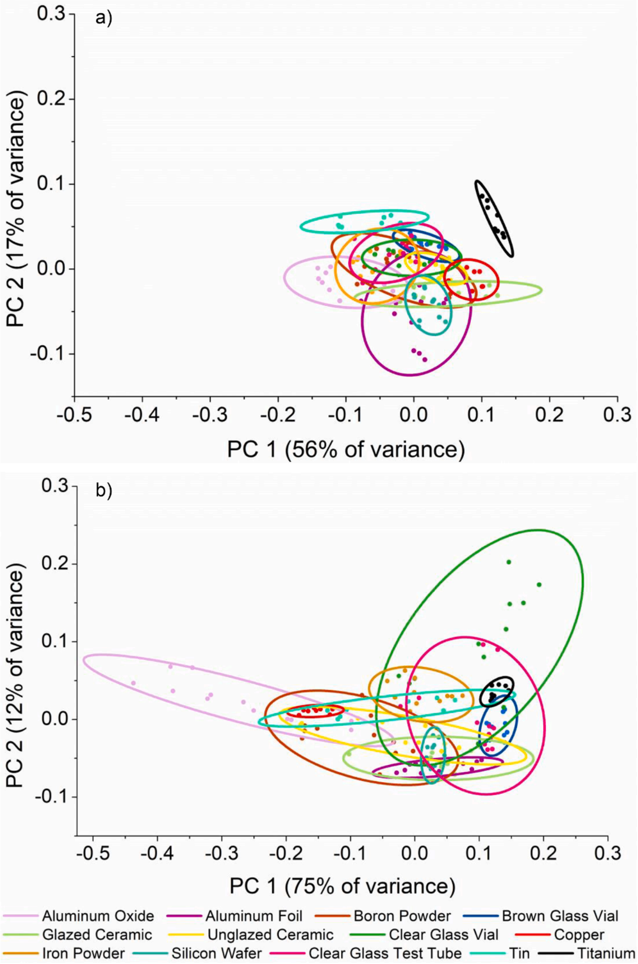

Fig. 6. Plots of scores for the first two principal components for a) positive ions and b) negative ions with circles showing a 95% confidence interval for each set of samples.

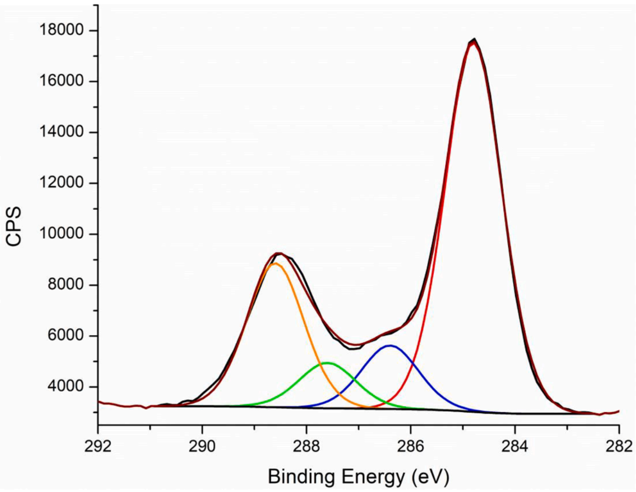

Fig. 7. C 1 s spectrum of adventitious carbon on titanium metal (with a passive titanium oxide film).

The amount of error introduced by neglecting beta shifts can be significant. Simulated AdC spectra were created based on real and plausible ratios of oxygen functionalities. When allowing the C–C peak to remain at 284.8 eV, the position of the main spectra peak maximum was seen to shift up to 0.2 eV or more (illustrated in Fig. 2). This observed shift likely accounts for some of the range of error noted in the previous work.[27].

The magnitude of the main peak shift appears to mainly depend on the amount of oxygen functionality overall. We created simulated spectra where the percentage of hydrocarbon remained the same and the ratios of the oxygen functionalities were changed. The C–C/C–H peak was positioned at 284.8 eV. In these experiments, the amount that the main peak maximum of the C 1 s spectrum shifted was very similar amongst samples with the same percentage of hydrocarbon, regardless of types of oxygen functionalities. The average main peak maximum of the simulated adventitious carbon with 10 %, 20 %, and 30 % oxygen-functionalized carbon was positioned at 284.84 eV, 284.88 eV, and 284.92 eV respectively. These values had very small standard deviations (less than 0.01 eV). One interesting observation regarding this data is that the shift appears to increase by approximately 0.04 eV each time 10 % more oxygen is added.

An adventitious carbon sample that has a higher percentage of hydrocarbon contribution can still have a significant shift in the main peak if it has a large proportion of C = O and O-C = O functionalities, as these beta carbons have a larger chemical shift (0.4 eV) than C-O beta carbons (0.2 eV). Unusually high amounts of C = O functionalities in particular can affect the peak position drastically, as the C = O beta peak is shifted more than the C-O beta peak and it has a larger ratio of beta to alpha carbons than the C-O and O-C = O beta peaks. Large amounts of O-C = O functionalities can also impact magnitude of shift for similar reasons.

This beta carbon peak model was tested on 117 samples with high-resolution XPS data acquired at Surface Science Western (SSW) at The University of Western Ontario (Western University) over a 5 year period from January 1, 2017 to December 31, 2021 (same data set as reference [27]). These samples were fit with the beta peak fitting model and charge corrected to an internal reference, such as a metallic peak, other conductive or semiconductive species, or other well-defined component. The position of the aliphatic C 1 s peak was recorded for each sample to determine its position relative to 284.8 eV.

On average, the aliphatic (C–C, C–H) peak was found to be positioned at 284.81 eV when using this method. This shift of 0.01 eV from the expected value of 284.8 eV is less than the error in the calibration of the spectrometer (+/- 0.025 eV). When compared to previous calculations using the traditional fitting method, which found an average shift of 0.11 eV,[27] this model provides an improvement in the deviation of the peak position. This fine-tuning of the position of the hydrocarbon peak allows for increased precision in charge referencing in AdC and this evidence should ease concerns that the position of the aliphatic peak position has been arbitrarily chosen, as it has now been cross-referenced using samples with internal secondary references. The generally accepted choice of using 284.8 eV for the aliphatic carbon position of AdC for charge correction purposes is valid.

The standard deviation of the peak position remains at 0.25 eV using this method for these 117 samples. As stated in reference [27], a portion of this deviation is likely due to the internal references themselves. While some internal references are well established with precisely known binding energies, others are less well known or complicated by contamination. The average calculated error of the internal references from reference [27] was 0.14 eV, with a median of 0.10 eV, a minimum of 0.025 eV, and a maximum of 0.7 eV. There are also small standard deviations associated with the beta carbon chemical shifts themselves. These are approximately 0.07 eV for the C*-C = O peak and 0.06 eV for the C*-(C = O)-O peak (due to the data available in Beamson and Briggs' XPS Polymer Handbook, we were unable to calculate a standard deviation for the C*-C-O peak). These various errors/standard deviations likely account for much of the error seen in our beta peak fitting model and in the standard fitting model from reference [27]. Other deviations in the positioning of the AdC C 1 s peak can be caused by the substrate and include work function effects and vacuum level (VL) alignment effects.[9].

3.3. Average adventitious carbon spectra

An average adventitious carbon spectrum was created by normalizing and aligning the binding energy axes of 80 adventitious carbon spectra from various material classes (same dataset as used in reference [27]) and averaging each point. The main peak of each spectrum was set to 284.8 eV, following the traditional fitting parameters for adventitious carbon. The average was determined to be reached when the spectral envelope did not significantly change with the addition of 10 more spectra. The result of this process is shown in Fig. 3 and Table 5.

One additional point noted from the average AdC C 1 s spectrum and from inspection of AdC spectra in general is the noted lack of any shake-up structures being present. If any significant alkene or aromatic functionality was present these structures would also need to be seen, generally in the 290 eV to 293 eV range. C = O functionality has generally weaker shake-up structures and is usually not seen as they are lost in the inelastic loss structure above the C 1 s region (e.g. for poly (vinyl methyl ketone) the shake-up structure is around 299 eV to 301 eV).[33].

These fitting parameters (Table 5) can be used to separate the contributions of adventitious and intrinsic carbon to the C 1 s spectrum. Fig. 4 shows an example of this, with a complex organic sample containing N-heterocyclic carbenes (NHC). The sources of carbon in this sample are an intermediate NHC, an end product NHC, and adventitious carbon. The presence of AdC made it difficult to determine the amount of each organic product from the C 1 s spectrum. Peak fitting components (area ratios, peak B.E. positions, FWHM) were developed for each of the intermediate and end product NHCs using their known chemistries. Peak positions for these were based on binding energies from a survey of similar functional groups. When the average adventitious carbon fitting was applied to the spectrum, it was possible to determine which portion of the spectrum originated from the sample as opposed to AdC. The amounts of AdC carbon versus the amount of NHC related carbon derived from the fitted C 1 s spectrum matched that of calculations of the amount of AdC derived from the survey spectrum data (N:C or O:C ratios) and the chemistry of the NHC compounds (see Table 6), showing that this is an effective tool for the XPS analysis of organic materials.[36].

As with XPS, an average adventitious carbon spectrum was created for ToF-SIMS (140 spectra total from 13 separate samples). This was done in a similar fashion to the XPS spectrum. The data was normalized to total selected ion counts (i.e. total counts for AdC ion fragments). Fig. 5 and Table 7 show the results of this process. These spectra can be used in a similar way to the XPS spectrum seen above.

The major hydrocarbon $C_xH_y^+$ ions at *m/z* 29 ($C_2H_5^+$), 41 ($C_3H_5^+$), 43 ($C_3H_7^+$) and 55 ($C_4H_7^+$) have the same nominal *m/z* values as CHO^+, C_2HO^+, $C_2H_3O^+$ and $C_3H_3O^+$. In S3 we show their spectra in expanded scales[37] for three different samples (Al foil, Cu sheet and Si wafer as examples) to show that the two types of ions with same nominal *m/z* values are well separated. We include in Fig. 5 and Table 7 peaks for CHO^+, $C_2H_3O^+$, and $C_3H_3O^+$ at *m/z* 29, 43, and 55 to account for their overlapping contributions with those of $C_2H_5^+$, $C_3H_7^+$, and $C_4H_7^+$, respectively. The amount of C_2HO^+ (*m/z* 41) seen in the AdC spectrum is negligible.

One additional takeaway from these average adventitious carbon spectra is further evidence that adventitious carbon is not graphitic in nature. Generally, the negative ion spectrum of graphite has C_n^- fragments that have approximately equal or greater intensity than their corresponding C_nH^- fragments,[38] due to graphite's low hydrogen content. This is not seen in our ToF-SIMS adventitious carbon spectra. In fact, the fragmentation pattern of the adventitious carbon spectra aligns more with that of a polymer (e.g. polyethylene, polypropylene) which always show a greater C_nH^- intensity than C_n^-.[39] This observation is consistent with our findings through XPS.

3.4. Principal component analysis of adventitious carbon ion fragments

Principal component analysis was performed separately on the positive and negative ion peak areas of adventitious carbon samples. In both cases, the first two PCs captured the majority of the variance in the dataset (73 % for positive ions, 68 % for negative ions). Fig. 6 shows the scores of these analyses with a 95 % confidence circle around each sample.

The positive PCA analysis shows many similarities in the adventitious carbon samples, as seen by the excessive overlap of the samples. This is expected, as most adventitious carbon is assumed to be similar. One interesting outlier is titanium-grown adventitious carbon (note sample surface is a passive titanium oxide film), which is situated in the upper right quadrant with no overlap with any other samples. This indicates that it is significantly different from the rest of the samples. We see this difference in the C 1 s XPS spectra as well, which have a very large carboxyl peak compared to other samples, as seen in Fig. 7. This extreme deviation from the normal composition of AdC suggests that this sample may not contain entirely adventitious carbon, some chemistry may have occurred between the carbon and the surface, or there is some preferential absorption of carboxyl containing species to this surface. In fact, it has been reported that TiO_2 selectively adsorbs carboxylic acid from air, while repelling other chemicals such as alcohols.[40] Other work showing large carboxyl peaks due to the presence of TiO_2 include a Au/TiO_2 catalyst,[41] sputtered TiO_2 thin films[42] and air-exposed Ti surfaces with obvious oxide films.[9] At the same time, the C 1 s spectrum of adventitious carbon for a titanium-based alloy (Ti-6AL-4 V) exposed to air may well have a shape characteristic of the average adventitious carbon C 1 s spectrum.[43] Reference [9] also shows similar carboxyl (and possibly carbonate) accumulation in the oxides of zirconium, manganese and yttrium. XPS users should be wary of an unusual shape of the adventitious carbon C 1 s peak and identify when there may be additional chemistries appearing.

The negative ion PCA conveys largely the same information. There does not appear to be any specific correlations or groupings between AdC on different material types. There are some samples that contain replicates with vastly different scores. This is likely due to the inevitable geometry effects associated with these samples, but this does not affect the conclusion substantially as they are still largely overlapping.

These results prove the general consistency of adventitious carbon for the samples selected for this study. Although it may differ slightly between surfaces, its chemistry is largely similar across samples.

4. Conclusions

As XPS becomes an increasingly popular method of sample characterization for many different types of chemistry, it is important to re-evaluate methodologies and prove the accuracy of the technique. This paper has advanced this endeavour from various angles, including investigating the chemical nature and origin of adventitious carbon. There are several important takeaways from this case study involving samples analyzed in our facility, including:

1) The observations from the D-parameter results and analysis of ToF-SIMS spectra confirms that AdC is not graphitic in nature. It is not appropriate to assign AdC a peak position of 284.5 eV, the binding energy of graphitic carbon. AdC is mainly aliphatic in nature.
2) An AdC fitting method that considers contributions from beta carbons was created to address one potential source of error in the charge referencing technique. This model was informed by vapour pressures and chemical configurations of various (mainly aliphatic) VOCs, which we believe is the most common source of AdC. Using this method, the average C–C/C–H AdC peak position was shown to be 284.81 eV (+/- 0.25 eV) via verification with a secondary internal reference. This is an improvement from previous work, which showed an average aliphatic peak position of 284.91 eV (+/-0.25 eV).[27] These findings indicate that, in order to be as accurate as possible, XPS users may wish to use the beta peak model to fit their C 1 s spectrum and charge correct the C–C/C–H peak position (as opposed to the main AdC peak maximum) to 284.8 eV. XPS literature B.E. accuracy may be improved if the XPS community coordinated to use this model as the standard for AdC charge referencing.
3) A presented average AdC spectrum is useful in the analysis of complex organic systems, as shown through peak fitting models of a real-world sample. This average spectrum can be used to deconvolute C 1 s high resolution spectra of organic materials where removal of surface adventitious carbon is not feasible. On average, ~ 25 % of the carbon species in AdC is directly associated with oxygen functionality.
4) Principal component analysis performed on ToF-SIMS spectra of AdC showed very little difference between AdC samples on various surfaces. Importantly, there was no grouping of material classes (e.g. metals, glasses, semi-conductors, powders, etc.). These results should mitigate concern that deposition of AdC on different surfaces will significantly affect the accuracy of this charge referencing practice. Average AdC ToF-SIMS spectra were also presented.

Declaration of competing interest

The authors declare that they have no known competing financial interests or personal relationships that could have appeared to influence the work reported in this paper.

Data availability

Data will be made available on request.

Acknowledgement

Funding for this project was provided by an NSERC (Natural Science and Engineering Research Council of Canada) Discovery Grant and a Western University Strategic Support for NSERC Success Seed Grant. The authors wish to thank Ms. Ekrupe Kaur and Dr. Yolanda Hedberg for permission to show Fig. 4 from their work. That work is affiliated with the Carbon to Metal Coating Institute at Queen's University (Kingston, Canada) and was partially funded by the NFRF-T (New Frontiers in Research Fund - Transformation, Social Sciences and Humanities Research Council, Canada) program (#NFRFT-2020-00573). The authors thank Dr. Jonas Hedberg for help with the chemometrics (PCA) software and Ms. Charlie Dearing for proofreading and editing support.

Appendix A. Supplementary data

Supplementary data to this article can be found online at https://doi.org/10.1016/j.apsusc.2024.159319.

References

[1] J.F. Moulder, W.F. Stickle, P.E. Sobal, K.D. Bomben, Handbook of X-ray Photoelectron Spectroscopy, Perkin-Elmer Corp., Eden Prairie, MN, 1992, pp. 22-23.
[2] G.B. Hoflund, Spectroscopic Techniques: X-ray Photoelectron Spectroscopy, Auger Electron Spectroscopy, and Ion Scattering Spectroscopy, in: J.C. Rivière, S. Myhra (Eds.), Handbook of Surface and Interface Analysis, Marcel Dekker Inc., New York, 1998, pp. 69–71.
[3] M.A. Kelly, Analysing Insulators with XPS and AES, in: D. Briggs, J.T. Grant (Eds.), Surface Analysis by Auger and X-Ray Photoelectron Spectroscopy, IM Publications, 2003, pp. 191–210.
[4] ASTM International, Standard Guide to Charge Control and Charge Referencing Techniques in X-Ray Photoelectron Spectroscopy, West Conshohocken, PA, 2016.
[5] D.R. Baer, K. Artyushkova, H. Cohen, C.D. Easton, M. Engelhard, T.R. Gengenbach, G. Greczynski, P. Mack, D.J. Morgan, A. Roberts, J. Vac. Sci. Technol. A. 38 (2020) 031204.
[6] J. Cazaux, J. Electron Spectros. Relat. Phenom. 113 (2000) 15.
[7] G. Barth, R. Linder, C. Bryson, Surf. Interface Anal. 11 (1988) 307.
[8] J.B. Metson, Surf. Interface Anal. 27 (1999) 1069.

[9] G. Greczynski, L. Hultman, Progr, Mater. Sci. 107 (2020) 100591.
[10] ASTM E1523-15 "Standard Guide to Charge Control and Charge Referencing Techniques in X-ray Photoelectron Spectroscopy" ASTM International, West Conshohocken PA USA.
[11] NIST X-ray Photoelectron Spectroscopy Database, NIST Standard Reference Database Number 20, National Institute of Standards and Technology, Gaithersburg MD, 20899 (2000), DOI: https://dx.doi.org/10.18434/T4T88K, (retrieved November 24, 2023).
[12] G. Greczynski, L. Hultman, J. Appl. Phys. 132 (2022) 011101.
[13] T.L. Barr, S. Seal, J. Vac. Sci. Technol. A. 13 (1995) 1239.
[14] J.C. Lascovich, R. Giorgi, S. Scaglione, Appl. Surf. Sci. 47 (1991) 17.
[15] D.J. Morgan, J. Carbon Res. 7 (2021) 51.
[16] G. Greczynski, L. Hultman, Vacuum. 205 (2022) 111463.
[17] H. Wang, L. Nie, J. Li, Y. Wang, G. Wang, J. Wang, Z. Hao, Chin. Sci. Bull. 58 (2013) 724.
[18] J. Xu, M. Szyszkowicz, B. Jovic, S. Cakmak, C.C. Austin, J. Zhu, Atmos. Environ. 141 (2016) 523.
[19] M.A. Bari, W.B. Kindzierski, A.J. Wheeler, M.-È. Héroux, L.A. Wallace, Build. Environ. 90 (2015) 114.
[20] Y. Liu, M. Shao, L. Fu, S. Lu, L. Zeng, D.
[21] S.C. Lee, M.Y. Chiu, K.F. Ho, S.C. Zou, X. Wang, Chemosphere 48 (2002) 375.
[22] J.F. Pankow, W. Luo, D.A. Bender, L.M. Isabelle, J.S. Hollingsworth, C. Chen, W. E. Asher, J.S. Zogorski, Atmos. Environ. 37 (2003) 5023.
[23] M.F. Mohamed, D. Kang, V.P. Aneja, Chemosphere 47 (2002) 863.
[24] M.I. Khoder, Atmos. Environ. 41 (2007) 554.
[25] Council Directive 2010/75/EU of the European Parliament and of the Council of 24 November 2010 on industrial emissions (integrated pollution prevention and control). Official Journal of the European Union. L334 (2010) 17-119.
[26] J.R. Rumble (Ed.), CRC Handbook of Chemistry and Physics, 103rd ed., CRC Press, Boca Raton, FL, 2022.
[27] M.C. Biesinger, Appl. Surf. Sci. 597 (2022) 153681.
[28] P. Swift, Surf. Interface Anal. 4 (1982) 47.
[29] B.V. Crist, J. Electron Spectrosc. Relat. Phenom. 231 (2019) 75.
[30] G. Greczynski, L. Hultman, Sci Rep. 11 (2021) 11195.
[31] F.A. Stevie, R. Garcia, J. Shallenberger, J.G. Newman, C.L. Donley, J. Vac. Sci. Technol. A. 38 (2020) 063202.
[32] N. Fairley, V. Fernandez, M. Richard-Plouet, C. Guillot-Deudon, J. Walton, E. Smith, D. Flahaut, M. Greiner, M. Biesinger, S. Tougaard, D. Morgan, J. Baltrusaitis, Appl. Surf. Sci. Adv. 5 (2021) 100112.
[33] G. Beamson, D. Briggs, High Resolution XPS of Organic Polymers: The Scienta ESCA300 Database, New York NY, 1992.
[34] D. Graham, Multivariate Analysis, NESAC/BIO. (2014). https://depts.washington.edu/nesacbio/mvsa/multivariate-surface-analysis-homepage (accessed March 21, 2023).
[35] M.C. Biesinger, P.-Y. Paepegaey, N.S. McIntyre, R.R. Harbottle, N.O. Petersen, Anal. Chem. 74 (2002) 5711.
[36] E. Kaur, M. Aloisio, D. Nanan, C. Crudden, Y.S. Hedberg, M.C. Biesinger, unpublished data, 2023.
[37] Y.-J. Zhu, N. Olson, T.P. Beebe Jr., Environ. Sci. Technol. 35 (2001) 3113.
[38] W. Xie, L.-T. Weng, K.L. Yeung, C.-M. Chan, Surf. Interface Anal. 50 (2018) 851.
[39] H.-Y. Nie, J. Vac. Sci. Technol. B 34 (2016) 030603.
[40] J. Balajka, M.A. Hines, W.J.I. DeBenedetti, M. Komora, J. Pavelec, M. Schmid, U. Diebold, Science 361 (2018) 786.
[41] S. Chenakin, N. Kruse, J. Catal. 358 (2018) 224.
[42] F. Güzelçimen, B. Tanören, Ç. Çetinkaya, M.D. Kaya, H.İ. Efkere, Y. Özen, D. Bingöl, M. Sirkeci, B. Kınacı, M.B. Ünlü, S. Özçelik, Vacuum 182 (2020) 109766.
[43] M.A. Vasylyev, S.P. Chenakin, L.F. Yatsenko, Acta Mater. 60 (2012) 6223.